Adsorption of Cyclic Ketones on the External and Internal Surfaces of a Faujasite Zeolite (CaX). A Solid-State ^{2}H NMR, ^{13}C NMR, FT-IR, and EPR Investigation

Nicholas J. Turro,*,† Xuegong Lei,† Wei Li,†,‡ Zhiqiang Liu,† and M. Francesca Ottaviani§

Contribution from the Department of Chemistry, Columbia University, New York, New York 10027, and Institute of Chemical Sciences, University of Urbino, 61029 Urbino, Italy

Abstract: The adsorption characteristics (binding distributions, location, interactions, supramolecular structures, kinetics) of two cyclic ketones, 2-phenylcyclododecanone ($\mathbf{1}_{12}$) and 2-phenylcyclopentadecanone ($\mathbf{1}_{15}$) onto the faujasite zeolite CaX have been investigated by a combination of spectroscopic techniques (^{2}H NMR, EPR, ^{13}C NMR, IR). This approach allows a detailed description of the supramolecular structure of the ketone@CaX complexes, the time dependence of exchange between binding sites, and the interactions of the ketones with coadsorbed molecules on the external and internal surface of CaX. It was found that, at room temperature, the smaller ketone, $\mathbf{1}_{12}$, readily enters the internal zeolite surface, whereas the larger ring ketone, $\mathbf{1}_{15}$, initially resides on the external surface but is adsorbed slowly into the internal surface. The results demonstrate that both $\mathbf{1}_{12}$ and $\mathbf{1}_{15}$ undergo a significant loss of mobility upon entering the CaX internal surface. Coadsorption of $\mathbf{1}_{12}$ and benzene into CaX results in a decrease in the mobilities of both $\mathbf{1}_{12}$ and benzene due to the fact that both benzene and $\mathbf{1}_{12}$ are adsorbed in the same supercage. On the contrary, it was found that $\mathbf{1}_{12}$ molecules negligibly perturbed the adsorption of nitroxide radicals, which are adsorbed exclusively on the external CaX surface. $\mathbf{1}_{15}$, which is initially adsorbed mainly at the external zeolite surface, undergoes progressive adsorption into the internal surface, which is accelerated by sample heating and increased loading. Coadsorption of $\mathbf{1}_{15}$ and benzene to CaX forces benzene molecules to aggregate in the supercages, because the benzene and $\mathbf{1}_{15}$ molecules in the internal surface cannot share the same supercage due to the large size of the $\mathbf{1}_{15}$ molecules. $\mathbf{1}_{15}$ also causes the aggregation of nitroxides that are adsorbed on the external surface. However, as $\mathbf{1}_{15}$ is adsorbed into the internal surface of CaX, the nitroxides deaggregate on the external surface sites. Radical scavenging of nitroxides adsorbed on the external surface of CaX occurred upon photolysis of $\mathbf{1}_{15}$@CaX but not upon photolysis of $\mathbf{1}_{12}$@CaX. The results are consistent with the model employed for the interpretation of the photochemistry of $\mathbf{1}_{12}$@CaX and $\mathbf{1}_{15}$@CaX.

Introduction

Faujasite (FAU) zeolites X and Y have been extensively used as microreactors in industrial and basic research laboratories interested in the catalytic and separation sciences.[1-4] Catalysis by zeolites depends on the properties of supramolecular structures and dynamics produced by adsorbed guest molecules, the compositional and structural characteristics of the zeolites (Si/Al ratio, framework, degree of hydration), and the charge-compensating cations (size, number, position, charge).

† Columbia University.

‡ Present address: Department of Pharmaceutical Sciences, University of Tennessee, Memphis, TN 38163.
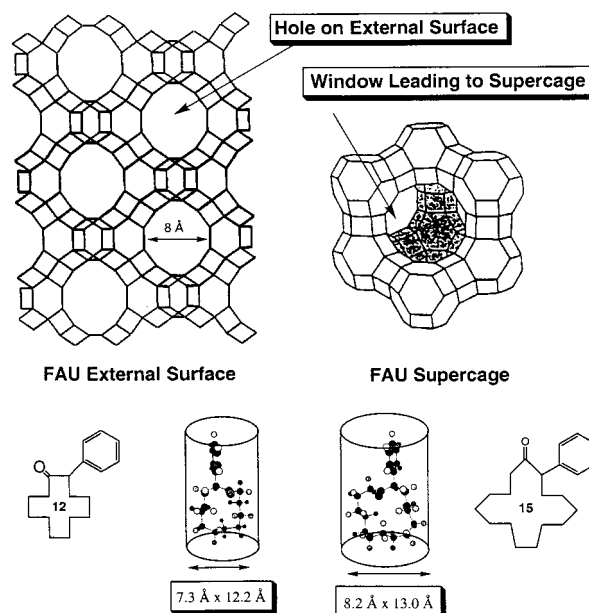
§ University of Urbino.

(1) (a) Davis, M. E. *Acc. Chem. Res.* **1993**, *26*, 111. Moscou, L. In *Studies in Surface Science and Catalysis 58*; Van Bekkum, H., Flanigen, E. M., Jansen, J. C., Eds.; Based on proceedings of the Summer School on Zeolites held in 1989 at Zeist, The Netherlands, 1991; p 1. Weisz, P. B. *Pure Appl. Chem.* **1980**, *52*, 2091. (b). Weisz, P. B. *Ind. Eng. Chem. Fundam.* **1986**, *25*, 53.

(2) Abrams, L.; Corbin, D. *J. Inclusion Phenom. Mol. Recognit. Chem.* **1995**, *21*, 1.

(3) Barrer, R. M. In *Inclusion Compounds*; Atwood, J. L., Davies, J. E. D., MacNicol, D. D., Eds.; Academic Press: New York, 1984; Vol. 1, p 191.
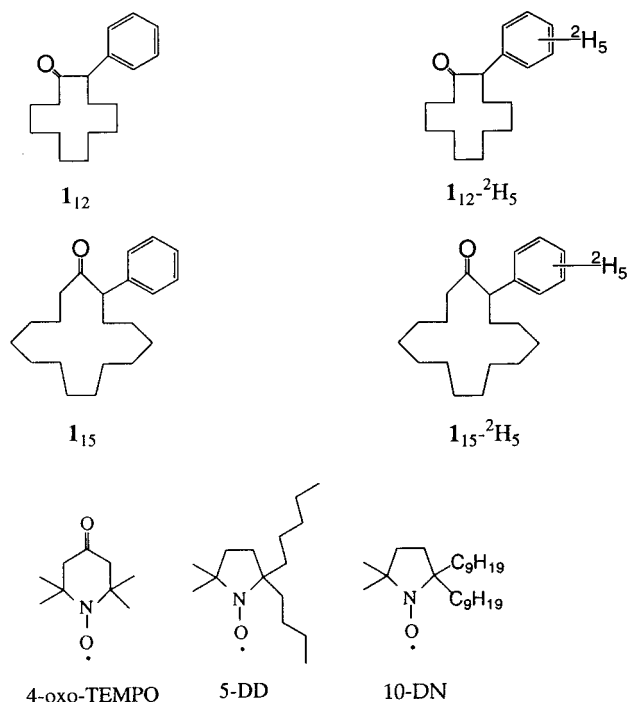
(4) Townsend, R. P. In *Studies in Surface Science and Catalysis 58*; Van Bekkum, H., Flanigen, E. M., Jansen, J. C., Eds.; Based on proceedings of the Summer School on Zeolites held in 1989 at Zeist, The Netherlands, 1991; p 359.

Chart 1

The void space structure (Chart 1) of NaX, a representative faujasite zeolite, consists of an interconnecting three-dimensional
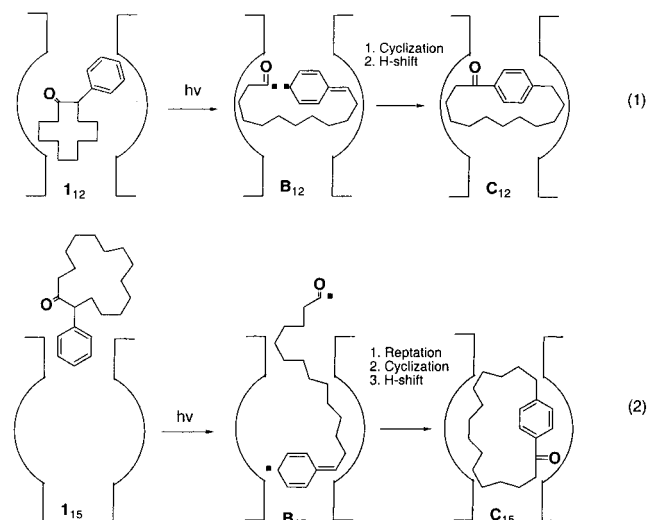
Chart 2

Scheme 1

structure and dynamics of the 1_{12}@CaX and 1_{15}@CaX complexes and to correlate the conclusions concerning the supramolecular structure and dynamics with the photochemical results.

A computer analysis of the lowest energy conformations of 1_{12} and 1_{15} (Chart 1) allows an evaluation of the maximum length and width (effective molecular cross section) of these molecules. On the basis of these cross sections and the size of the external pores on the surface of FAU zeolites (Chart 1), the smaller 1_{12} molecules are expected to pass through the 8-Å pores on the external surface of CaX more readily than the larger 1_{15} molecules at room temperature.[7] However, it is a priori plausible that 1_{15} molecules may enter the CaX internal surface through conformational changes of the relatively flexible cycloalkyl chain, which would allow slow adsorption and transport through the pores on the external surface at room temperature. Finally, it is expected that the rate at which 1_{15} enters the internal surface should depend on experimental conditions such as temperature and loading. The spectroscopic method allows both a direct and indirect investigation of these issues.

To investigate the different adsorption sites and the time profile of adsorption of the ketones, we have examined spectroscopically the adsorption of 1_{12}@CaX and 1_{15}@CaX, in the absence and in the presence of different host molecules that are unambiguously located on either the internal (benzene) or on the external (nitroxides) surface.

^{2}H NMR is a useful spectroscopic tool for directly acquiring information about the motion and the environmental properties of adsorbed molecules and the interaction of adsorbed guests with host systems.[9] Therefore, a ^{2}H NMR investigation of selectively deuterated 1_{12} and 1_{15} (structures in Chart 2) was undertaken in order to provide direct structural and dynamic information on 1_{12}@CaX and 1_{15}@CaX. In addition, further information on structure and adsorbate dynamics could be obtained by a ^{2}H NMR study of coadsorbed deuterated benzene ($C_6{}^2H_6$) and 1_{12}@CaX (or 1_{15}@CaX). Computer simulations of ^{2}H NMR spectra and their comparison to experimental spectra[9] provide detailed information on the supramolecular structure and dynamics of the adsorbed molecules at different sites as a function of time. Thus, ^{2}H NMR of $C_6{}^2H_6$ provides an indirect probe of 1_{12} and 1_{15}, which enter the internal surface, and a direct probe of the structure and dynamics of benzene @CaX in the presence and absence of 1_{12} and 1_{15}.

The analysis of electron paramagnetic resonance (EPR) spectra of nitroxide spin probes provides very precise structural

network that possesses 8-Å pore openings on the external surface and 13-Å internal supercages connected by 8-Å pores.[5] Charge-compensating cations occupy three different sites[5] (termed SI, SII, and SIII sites) of the internal surface. In particular, cations at SII (in the channels between supercages) and SIII (in the supercages) are accessible for significant interactions with adsorbed guest molecules. Molecules located at SIII in the supercages are more mobile than those located at SII. The exchange of Na^+ with Ca^{2+} is usually incomplete.[6] Sites are preferentially replaced by Ca^{2+} in the order of SI > SII > SIII. When the population of Ca^{2+} in SII is greater than 75%, the framework of CaX is slightly distorted so that not all supercages and pores (including those on the external surface) have the same size. In particular, this means that some pores on the external surface are slightly larger than the others.

A photochemical investigation of the two ketones (structures shown in Chart 2), 2-phenylcyclododecanone (1_{12}) and 2-phenylcyclopentadecanone (1_{15}), adsorbed on CaX (1_{12}@CaX and 1_{15}@CaX, respectively) has been reported.[7,8] Extraction experiments indicated that at room temperature 1_{12} is adsorbed mainly on the internal surface and that 1_{15} is adsorbed mainly on the external surface.[7] Although the initial siting of the two ketones was different, the course of the photochemistry led to structurally related cyclophane products (Scheme 1), C_{12} and C_{15}, through the intermediacy of biradicals, B_{12} and B_{15}. To test this model of the photochemistry, we report the use of several spectroscopic methods (NMR, EPR, IR), in addition to computational methods in simulating spectra, to obtain insight to the supramolecular

(5) Breck, D. W. *Zeolite Molecular Sieves*, Wiley: New York, 1974.

(6) Lei, G.-D.; Kevan, L. *J. Phys. Chem.* **1990**, *94*, 6384.

(7) Lei, X.-G.; Doubleday, C., Jr.; Zimmt, M. B.; Turro, N. J. *J. Am. Chem. Soc.* **1986**, *108*, 2444. Lei, X.-G.; Doubleday, C., Jr.; Turro, N. J. *Tetrahedron Lett.* **1987**, 4675.

(8) For discussions of supramolecular photochemistry in organized and confined media, see: (a) Weiss, R. G.; Ramamurthy, V.; Hammond, G. S. *Acc. Chem. Res.* **1993**, *26*, 530. (b) Ramamurthy, V.; Weiss, R. G.; Hammond, G. S. *Adv. Photochem.* **1993**, *18*, 69. For discussions and examples of photochemistry in zeolites, see: (c) Joy, A.; Ramamurthy, V. *Chem. Eur. J.* **2000**, *6*, 1287. (d) Turro, N. J. *Acc. Chem. Res.* **2000**, *33*, 637−646. (e) Scaiano, J. C.; Kaila, M.; Corrent, S. *J. Phys. Chem. B* **1997**, *101*, 8564.

(9) Klinowski, J., *Prog. NMR Spectrosc.* **1984**, *16*, 237.

and dynamic information about the probes and their environments.[10] Smaller nitroxide radicals, such as 4-oxo-Tempo (structure in Chart 2), can enter the internal structure of CaX and bind to different sites.[11,12] However, from experimental evidence to be presented below, larger nitroxide molecules, such as 5-doxyldecane (5-DD) and 10-doxylnonadecane (10-DN) employed in this study (structures in Chart 2), possess molecular cross sections that are too large for these molecules to enter the internal surface of CaX at room temperature. These nitroxides, therefore, are constrained to remain on the external surface. Computer-aided analysis of the nitroxide EPR spectra allows computation of parameters directly related to rotational mobility, environmental polarity, exchange rate among proximate radicals, and the fractions of the radicals that partition in different sites. Thus, EPR analysis of the coadsorption of nitroxides 5-DD and 10-DN will provide indirect probes of the supramolecular structure and dynamics of 1_{12} and 1_{15} molecules that are adsorbed on the external surface of CaX. It will be shown that, as in the case of ^{2}H NMR, EPR can also provide direct information on the interactions of 1_{12} and 1_{15} with coadsorbed materials and direct and indirect information on the time profiles of supramolecular structural reorganizations.

Finally, photolysis of the ketones in the presence of nitroxide molecules resulting in radical scavenging can modify the EPR spectral line shapes and intensities, providing still another in situ method to investigate the siting of the structures of 1_{12}@CaX and 1_{15}@CaX.

To summarize, this report will present a detailed ^{2}H NMR and EPR investigation of 1_{12}@CaX and 1_{15}@CaX, in the absence and in the presence of coadsorbed $C_6{}^2H_6$ and nitroxide radicals (5-DD, 10-DN). Further and complementary information is obtained by the use of ^{13}C NMR and FT-IR spectroscopy. The results will be compared to the interpretation of the photochemistry of 1_{12}@CaX and 1_{15}@CaX.

Experimental Section

Materials. 2-Phenylcyclododecanone (1_{12}) and 2-phenylcyclopentadecanone (1_{15}) were prepared following a procedure described elsewhere.[13] 2-Phenyl[^{2}H$_5$]cyclododecanone (1_{12}-^{2}H$_5$) and 2-phenyl[^{2}H$_5$]cyclopentadecanone (1_{15}-^{2}H$_5$) were synthesized by a modification of the published procedure[13] by using phenyl[^{2}H$_5$]lithium instead of phenyllithium. The structures and purity of the ketones were confirmed by GC/MS and ^{1}H and ^{13}C NMR analysis. 5-DD, 10-DN, and pentane (Aldrich) were used as received. CaX was either a gift from Dr. V. Ramamurthy or was prepared by exchange from NaX (Linde) by the procedure described in the literature.[6,14]

Sample Preparation. CaX was activated overnight on a vacuum line at 160−180 °C. The loading of individual guest molecules (ketone or nitroxide) onto CaX was performed by mixing the selected amounts of molecules (ketone or nitroxide) in 0.8 mL of pentane with 300 mg

(10) *Spin Labeling. Theory and Applications*; Berliner, L. J., Ed.; Academic Press: New York, 1976, 1979; Vol. 1., Vol. 2. (b) *Biological Magnetic Resonance. Spin Labeling, Theory and Applications*; Berliner L. J., Reuben, J., Eds.; Plenum Press: New York, 1989; Vol. 8.

(11) (a) Kasai, P.; Bishop, R. J., Jr. In *Zeolite Chemistry and Catalysis*; Rabo, J. A., Ed.; ACS Monograph 171; American Chemical Society: Washington, DC, 1976; p 350. (b) Romanelli, M.; Martini, G.; Kevan, L. *J. Phys. Chem.* **1986**, *84*, 4818; **1988**, *92*, 1958. (c) Martini, G.; Ristori, S.; Romanelli, M.; Kevan, L. *J. Phys. Chem.* **1990**, *94*, 7607. (d) Martini, G.; Ottaviani, M. F.; Romanelli, M. *J. Colloid Interface Sci.* **1987**, *115*, 87. (e) Mazzoleni, F.; Ottaviani, M. F.; Romanelli, M.; Martini, G. *J. Phys. Chem.* **1988**, *92*, 1953. (f) Romanelli, M.; Ottaviani, M. F.; Martini, G.; Kevan, L. *J. Phys. Chem.* **1989**, *93*, 317.

(12) Ottaviani, M. F.; Garcia-Garibay, M.; Turro, N. J. *Colloids Surf.* **1993**, *72*, 321.

(13) Lei, X.-G.; Doubleday, C., Jr.; Turro, N. J. *Tetrahedron Lett.* **1987**, 4671.

(14) Ramamurthy, V.; Corbin, D. R.; Johnson, L. J. *J. Am. Chem. Soc.* **1992**, *114*, 3870.
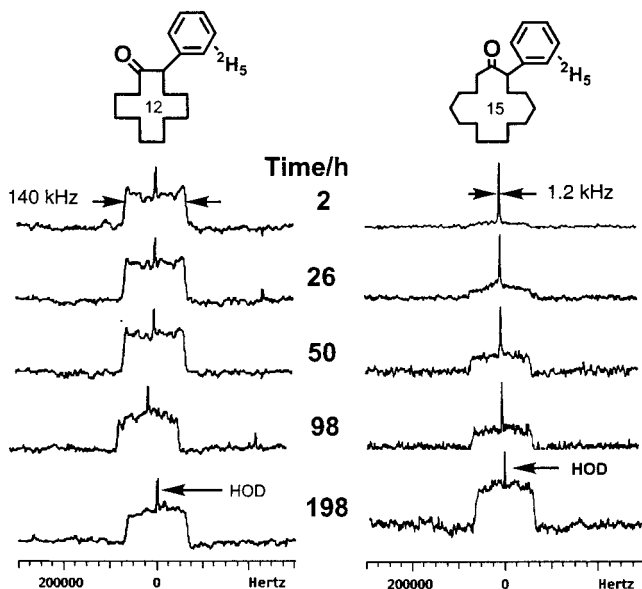
of activated zeolite. The mixture was stirred for 1 h and then dried under vacuum. All the samples were prepared in parallel, under the same conditions. For monitoring guest molecules externally and internally in the zeolite structure, the samples were flash eluted with pentane, and the eluted liquid was analyzed by GC with 1-phenyldodecane as the internal standard.

Coadsorbed mixtures of benzene and ketone samples were prepared as follows. A 350-mg sample of CaX was heated to 160 °C overnight under vacuum. A known amount of benzene was first adsorbed on CaX through the vapor phase and then a pentane solution containing a known amount of the ketone was added to the CaX. The solvent was removed by a stream of argon and then pumped under vacuum. The sample was transferred to a NMR cell for analysis. Coadsorbed mixtures of nitroxide and ketone were prepared in an analogous manner.

Photolysis. A 50-mg sample of zeolite loaded with 2 mg of ketone (termed 4 wt %/wt of guest to zeolite and abbreviated as percent loading throughout the text) was inserted in a quartz cell. The cell was rotated and irradiated under vacuum for 20 min with a 450-W medium-pressure mercury lamp equipped with a chromate solution filter (the conversion of the starting material was typically ~50%).

Instrumental Analysis. Solid-state ^{2}H NMR spectra were recorded on a Bruker 250-MHz NMR spectrometer at 38.397 MHz. A quadrupole echo sequence was employed at 3.4-μs (90°pulse) radio frequency pulses and 1-s recycle delays. The delay time between the two 90° pulses was 25 μs . The ^{2}H NMR spectra were simulated by means of the program Turbopowder kindly provided by Prof. A. McDermott (Columbia University, New York). ^{13}C cross polarization magic angle spinning (CP-MAS) solid-state NMR was recorded on a Bruker 250-MHz NMR spectrometer at 62.896 MHz with 6.2-μs radio frequency pulses and 2-s recycle delays (contact time of 2 ms and spinning rate of 4 kHz). EPR spectra were recorded on a Bruker ESP300 spectrometer interfaced to a computer with the ESP1600 software system. FT-IR spectra were recorded on a Perkin-Elmer 1800 infrared spectrophotometer.

Results and Discussion

Photochemistry of 1_{12}@CaX and 1_{15}@CaX. The photochemistry[7] of 1_{12}@CaX and 1_{15}@CaX results in the formation (Scheme 1, eqs 1 and 2) of cyclophanes C_{12} and C_{15}, respectively, as the major products. The formation of both cyclophanes is postulated to result from para coupling of biradical intermediates, B_{12} and B_{15} which, after a hydrogen shift, produces the cyclophanes, C_{12} and C_{15}, respectively. From solvent extraction experiments,[7] it was concluded that 1_{12} was initially adsorbed on the internal surface and that 1_{15} was adsorbed initially on the external surface. The biradical B_{12} undergoes cyclization to form C_{12} within a supercage of CaX (Scheme 1, eq 1). Since neither 1_{15} nor C_{15} was significantly adsorbed into the internal surface during the time scale of the photolysis (typically minutes), it was concluded that the biradical B_{15} is formed on the external surface and then diffuses ("reptates") into the internal surface (Scheme 1, eq 2). The latter result requires that the reptation of B_{15} into the internal surface is faster than the cyclization of B_{15} on the external surface. The results reported here were intended to test the validity of the proposed supramolecular mechanism for photolysis of 1_{12}@CaX and 1_{15}@CaX. In particular, the spectroscopic experiments described below were designed to investigate the supramolecular structure and dynamics of adsorption of 1_{12}@CaX and 1_{15}@CaX.

Solid-State ^{2}H NMR of 1_{12}-^{2}H$_5$@CaX and 1_{15}-^{2}H$_5$@CaX. The spectrum of 1_{12}-^{2}H$_5$ (Figure 1, left) showed a major component consisting of a broad band (width at half-height, $\Delta h_{1/2}$, ~140 kHz) and a very minor component consisting of a very narrow band ($\Delta h_{1/2}$ ~7 kHz). The broad peak is typical of a signal (vide infra) resulting from molecules being in the limit of slow motion ($\Delta h_{1/2}$, ~140 kHz) of ^{2}H NMR, while the narrow peak is typical of a signal (vide infra) that results from molecules

Figure 1. ^{2}H NMR spectra (room temperature) of $\mathbf{1}_{12}$-^{2}H$_5$@CaX (left) and $\mathbf{1}_{15}$-^{2}H$_5$@CaX (right) at 3% loading at different times after loading: (from the top) 2, 26, 50, 98, and 198 h. The sharp signal in all of the spectra of $\mathbf{1}_{12}$-^{2}H$_5$@CaX and in the long-time spectra of $\mathbf{1}_{15}$-^{2}H$_5$@CaX is assigned to HOD impurity (see text for discussion).

approaching the fast motion limit ($\Delta h_{1/2}$, $\sim$1 kHz) of ^{2}H NMR. In control experiments, the narrow, minor component signal was shown to result mainly from a small amount of HOD adsorbed by the sample. This signal will not be considered in the discussion of the results. The spectrum of $\mathbf{1}_{12}$-^{2}H$_5$, which was taken $\sim$1 h after sample preparation, did not change over time (up to $\sim$200 h, Figure 1).

In contrast to the very broad spectrum observed for $\mathbf{1}_{12}$-^{2}H$_5$ which did not change with time, the spectrum of $\mathbf{1}_{15}$-^{2}H$_5$, taken immediately after sample preparation, consisted (Figure 1, right) almost entirely of a sharp band ($\Delta h_{1/2}$, $\sim$2 kHz), which was slowly converted to a broad signal ($\Delta h_{1/2}$, $\sim$140 kHz) after $\sim$200 h. The sharp signal indicates that initially the $\mathbf{1}_{15}$-^{2}H$_5$ molecules were highly mobile and close to the fast motion limit of ^{2}H NMR. However, upon "aging" at room temperature for $\sim$24 h, a broad component appeared and increased both in line width and in intensity relative to the sharp peak, an indication that the $\mathbf{1}_{15}$-^{2}H$_5$ molecules are being transferred to an environment in which their motion is strongly constrained. After several weeks, the spectrum of $\mathbf{1}_{15}$-^{2}H$_5$@CaX (Figure 1, right bottom) appeared very similar to that of $\mathbf{1}_{12}$-^{2}H$_5$@CaX (Figure 1, left) immediately after preparation. As in the case of $\mathbf{1}_{12}$, a minor sharp signal that remained after many hours is assigned to a minor amount of HOD contamination. The broad spectrum resulting from "aging" of $\mathbf{1}_{15}$-^{2}H$_5$@CaX could be produced in a shorter time by increasing the temperature; i.e., the process was completed in 1 h at 90 °C.

The results shown in Figure 1 demonstrate that $\mathbf{1}_{12}$-^{2}H$_5$ molecules are mainly located, immediately after preparation at room temperature, in the internal CaX surface, whereas $\mathbf{1}_{15}$-^{2}H$_5$ molecules are initially adsorbed at the external surface of the zeolite. Furthermore, the spectra show that at room temperature $\mathbf{1}_{15}$-^{2}H$_5$ molecules slowly penetrate into the internal zeolite structure. Evidently, the 15-membered ring of $\mathbf{1}_{15}$ molecules is sufficiently flexible and/or some of the pore openings of CaX are sufficiently large (due to distortions from Ca^{2+} exchange or to occurrence of unexchanged Na$^+$) to allow the slow entrance of $\mathbf{1}_{15}$ molecules into the internal zeolite structure at room temperature. The motion of $\mathbf{1}_{15}$-^{2}H$_5$ molecules

on the external surface was nearly isotropic on the ^{2}H NMR time scale, corresponding to a correlation time for motion of $<10^{-7}$ s.[12,15] The spectra of $\mathbf{1}_{12}$-^{2}H$_5$@CaX (room temperature) and $\mathbf{1}_{15}$-^{2}H$_5$@CaX (heated to 90° C for several hours) had a broad line shape expected[16] for phenyl rings adsorbed with constrained motion in the internal CaX structure. This signal narrowed with an increase in temperature to 70° C, and this change was reversible (results not shown).

The adsorption of $\mathbf{1}_{15}$ from the external surface to the internal surface may be monitored directly by ^{2}H NMR from the ratio of the intensity of the sharp signal (external surface) to the broad signal (internal surface). The variation of the relative intensity of the sharp component with time for $\mathbf{1}_{15}$-^{2}H$_5$@CaX (3% loading) at 70 °C was investigated. Qualitatively, the time profile is bimodal, with approximately two-thirds of the ketone molecules being adsorbed into the internal surface at a relatively fast rate ($\sim$3 h) and the remainder being adsorbed at a slower rate ($\sim$15 h). The rate decrease in the adsorption process over a long time is not likely to be attributable to a "saturation" of the internal structure by the ketone, since a 3% loading of $\mathbf{1}_{15}$ corresponds to much less than 1 molecule of $\mathbf{1}_{15}$/supercage and a saturation loading is expected to be $\sim$15%.

The ^{2}H NMR spectra of $\mathbf{1}_{12}$-^{2}H$_5$ and $\mathbf{1}_{15}$-^{2}H$_5$ as a function of percent loading are shown in Figure 2. Qualitatively, the rate of adsorption of $\mathbf{1}_{15}$-^{2}H$_5$ into the internal surface increased with increasing loading, but the rate of adsorption of $\mathbf{1}_{12}$-^{2}H$_5$ was fast on the time scale of the measurements and not significantly affected by loading.

^{2}H NMR Spectra of Perdeuterated Benzene (C$_6$^{2}H$_6$) Absorbed on CaX in the Absence and in the Presence of $\mathbf{1}_{12}$ and $\mathbf{1}_{15}$. The adsorption of $\mathbf{1}_{12}$ and $\mathbf{1}_{15}$ on CaX was studied indirectly by monitoring the changes in the ^{2}H NMR spectra of coadsorbed perdeuterated benzene (C$_6$^{2}H$_6$). Figure 3a shows the ^{2}H NMR experimental spectra of C$_6$^{2}H$_6$@CaX, at 2% loading, in the absence and in the presence of $\mathbf{1}_{12}$ and $\mathbf{1}_{15}$ (both at 15% loading) at different delay times after coadsorption. For a 2% loading of benzene, there is much less than 1 benzene molecule/supercage on the average. The high (15%) loading of ketone was selected (Figure 2) to reduce the time of initial adsorption of $\mathbf{1}_{15}$ and to make this time comparable to the time of reorganization of benzene in the internal surface. If all of the ketone at 15% loading is adsorbed in the internal surface, there will be on average 1 ketone molecule/supercage.

It is generally accepted that up to 1−3 benzene molecules can be adsorbed at the SII sites in a supercage, due to the π-electron/cation interaction, and that a maximum of 5−6 benzene molecules can occupy a supercage.[17] The experimental spectra of Figure 3a were simulated (Figure 3b) by adding two components, corresponding to two types of motion of the benzene molecules:

(a) One component consists of jumps between the adsorption sites, such as site exchange in a supercage or among supercages. This motion is isotropic and results in a Lorentzian line shape at room temperature. This signal is termed the "isotropic component" of the spectra. The line width was set at 5 kHz for the spectra in the absence of ketones and in the presence of $\mathbf{1}_{12}$ (first and second columns, Figure 3b) and is indicated in parentheses for the spectra in the presence of $\mathbf{1}_{15}$ (third column, Figure

(15) Turkevich, J. *J. Catal. Rev.* **1968**, *1*, 1.
(16) Rice, D. M.; Meinwald, Y. C.; Scheraga, H. A.; Griffin, R. G. *J. Am. Chem. Soc.* **1987**, *109*, 1636.
(17) (a) Boddenberg, B.; Burmeister, R. *Zeolites*, **1988**, *8*, 488. (b) Burmeister, R.; Schwarz, H.; Boddenberg, B. *Ber. Bunsen-Ges. Phys. Chem.* **1989**, *93*, 1309.
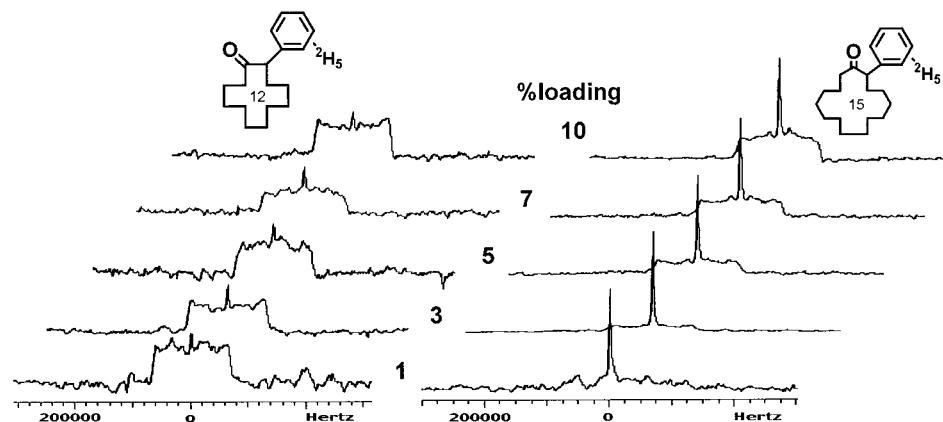
Figure 2. ^{2}H NMR spectra (room temperature) of 1_{12}-^{2}H$_5$@CaX (left) and 1_{15}-^{2}H$_5$@CaX (right) at different loadings (from the bottom) 1 (40 h), 3 (13 h), 5 (8 h), 7 (6 h), and 10% (4 h). The time required for acquisition of the spectra is given in parentheses next to the percent loadings.

3b). The jumping rate limit of 1×10^9 s^{-1} was assumed for the simulation.[18,19]

(b) The second component consists of fast 6-fold anisotropic rotation of the benzene ring about the π-electron/cation bond axis.[20] This results in a powder pattern with splitting of 69 kHz. The computation used half of the static quadrupole coupling constant, 180 kHz. The asymmetry parameter was 0.06 and the line width was 2 kHz.[21] This component is termed the "anisotropic component" of the spectra.

The ratio between the anisotropic component (normalized to intensity 1) and the isotropic component (termed W/N), which reproduced the experimental spectra, is reported beside each computed spectrum.

For the initial measurements (of the order of 1 h after sample preparation), the relative intensity of the anisotropic component was somewhat larger for the spectra in the presence of the cyclic ketones than in their absence. This means that, at the start of the measurements, the adsorption of the cyclic ketone causes a constraint of motion for some fraction of the benzene molecules in the internal CaX structure. The initial spectra are similar, except for the differences in ratio of isotropic to anisotropic components, but the time dependence of the spectra are different for the three systems, C$_6$^{2}H$_6$@CaX, C$_6$^{2}H$_6$/1_{12}@CaX, and C$_6$^{2}H$_6$/1_{15}@CaX. In the absence of ketones, the isotropic component increased upon aging (Figure 3b, left), indicating an increase in mobility of the benzene molecules with time. In contrast, the relative intensity of the anisotropic signal increased over time at the expense of the isotropic component when 1_{12} was coadsorbed, leaving behind only the anisotropic component (Figure 3b, middle), indicating a strong decrease in mobility with aging. A decrease in the intensity of the anisotropic component over time was found for the C$_6$^{2}H$_6$/1_{15}@CaX sample (analogous to the observation for C$_6$^{2}H$_6$/1_{12}@CaX), but the remaining component, while similar to that of the isotropic component, possessed a considerably broader line width (Figure 3b, right).

These results are interpreted in terms of an initial nonequilibrium distribution of benzene in the internal surface for the initial measurements, followed by redistribution of benzene

molecules depending on the situation (absence of ketones, coadsorption of 1_{12}, coadsorption of 1_{15}). At 2% loading, a homogeneous distribution of benzene within the internal surface would correspond to less than 1 benzene molecule/2 supercages. At 15% loading, a homogeneous distribution of ketones within the internal surface would correspond to ~1 ketone molecule/supercage.

With the above information in hand, the results shown in Figure 3 are interpreted in terms of the following supramolecular structure and dynamics of the benzene under the three following conditions:

(1) Behavior of Benzene in the Absence of Cyclic Ketones. We assume that all the benzene is initially internalized in the supercages, but in a nonequilibrium distribution in which the concentration of benzene molecules near the surface of the zeolite crystal is greater than that near the center of the zeolite crystal.[20] When benzene is initially deposited from the vapor phase onto CaX, some fraction of benzene molecules cluster together and aggregate in supercages near the external surface, and other benzene molecules diffuse and become more or less isolated in supercages in a nonequilibrium situation (e.g., Scheme 2, left). This initial condition corresponds to the simultaneous observation of an isotropic (supercage with one benzene molecule in fast motion) and an anisotropic (supercage with benzene aggregates in slow motion) component at the early times of observation. After a few hours, the system moves toward equilibrium as the benzene aggregates begin to break up and as benzene molecules diffuse into the center of the zeolite crystal to supercages that are unoccupied. With time, the aggregates decrease in number, the isotropic jumping between adsorption sites increases, and eventually, fast rotation of the benzene ring and averaging of the benzene motion occur, as most (or all) of the benzene molecules occupy a single supercage. At equilibrium, the anisotropic component disappears completely and the spectrum appears as a Lorentzian line (isotropic component), and the benzene molecules occupy individual supercages and enjoy isotropic motion.

(2) Behavior of Benzene in the Presence of 1_{12}. In this case, both 1_{12} and C$_6$^{2}H$_6$ are initially adsorbed in the internal surface, and the anisotropic component is somewhat larger than in the absence of 1_{12} because some supercages are occupied by 1_{12}, leaving fewer supercages for benzene adsorption and causing more benzene molecules to aggregate in the available supercages. As the benzene aggregates undergo redistribution together with the 1_{12} molecules, there is a progressive crowding of

(18) Wittebort, R. J.; Olejniczak, E. T.; Griffin, R. G. *J. Chem. Phys.* **1987**, *86*, 5411.

(19) Meier, P.; Kothe, G.; Jonsen, P.; Trecoske, M.; Pines, A. *J. Chem. Phys.* **1987**, *87*, 6867.

(20) (a) Lechert, H.; Basler, W. D.; Wittern, K.-P. Nuclear Relaxation Studies of Aromatics in Faujasite Type Zeolites, In *Proceedings of the 7th International Zeolite Conference*, Tokyo, 1986. (b) Lechert, H. *Catal. Rev.-Sci. Eng.* **1976**, *14*, 1.

(21) Greenfield, M. S.; Ronemus, A. D.; Vold, R. L.; Vold, R. R. *J. Magn. Reson.* **1987**, *72*, 89.
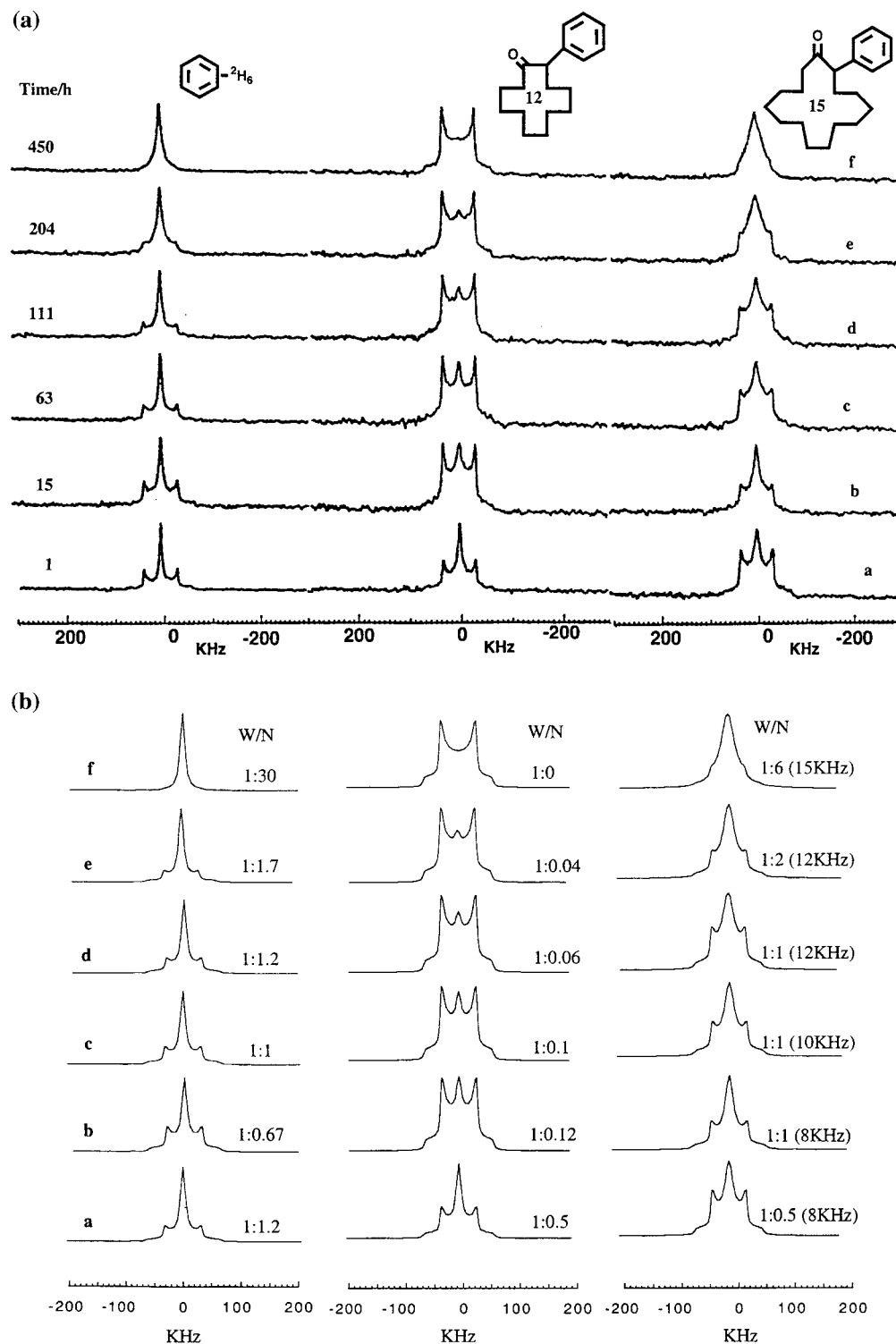
Figure 3. ^{2}H NMR spectra of perdeuterated benzene adsorbed onto CaX (2% loading) in the absence (left column) and in the presence of $\mathbf{1}_{12}$ (central column) and $\mathbf{1}_{15}$ (right column) (15% loading), recorded at different times after loading: (a) experimental spectra; (b) computed spectra.

benzene in the zeolite structure due to the presence of $\mathbf{1}_{12}$ molecules, which reduces the jumping rate among sites, giving rise to the progressive disappearance of the isotropic component. Eventually, benzene molecules become completely constrained by the ketone molecules that occupy supercages together with benzene molecules, and only the anisotropic component remains. Thus, the benzene−ketone interactions in supercages contribute to the progressive disappearance of the isotropic component over time. This conclusion is consistent with the simulated spectra shown in Figure 3b and is shown schematically in Scheme 2.

(3) Behavior of Benzene in the Presence of $\mathbf{1}_{15}$. The initial situation is similar to that found in the absence of ketone except that the percentage of the anisotropic component is slightly greater for those samples to which $\mathbf{1}_{15}$ has been coadsorbed. As in the absence of $\mathbf{1}_{15}$ molecules, the initial mixture of isotropic and anisotropic signals eventually is converted into a signal dominated by an isotropic contribution. However, the line width of the final isotropic component is larger than that for benzene alone. A plausible interpretation of this result is that, for a single supercage, several molecules of benzene occupy

Scheme 2
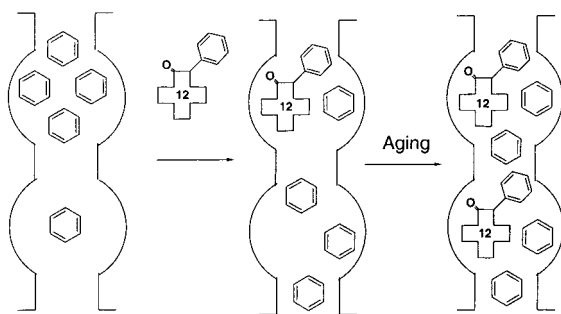
Scheme 3
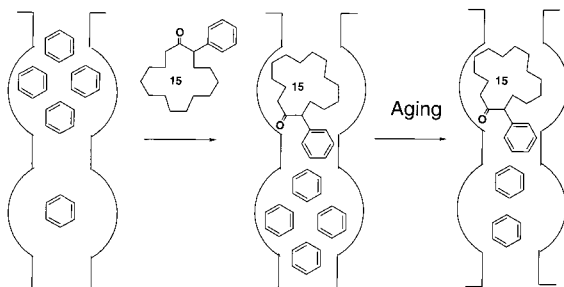
SII sites (the channels between supercages) but do not occupy supercages containing $\mathbf{1}_{15}$ molecules. Such a situation would favor collisions among benzene molecules in a site-exchange process, with a consequent line broadening (exchange broadening) in the spectra compared to the situation in the absence of $\mathbf{1}_{15}$. This conclusion is consistent with the simulations shown in Figure 3b and is shown schematically in Scheme 3.

EPR Spectra of Nitroxide Radicals in the Absence and Presence of $\mathbf{1}_{12}$ and $\mathbf{1}_{15}$. Figure 4 shows representative EPR spectra of 10-DN (structure shown in Chart 2) at 0.01 (Figure 4a) and 1% (Figure 4b) loading, in the absence and in the presence of $\mathbf{1}_{12}$ and $\mathbf{1}_{15}$ (5% loading), adsorbed onto CaX. The full lines are the experimental spectra (298 K), whereas the dashed lines are the simulated spectra.[22] The main parameters obtained from simulation are as follows:

(i) There are two sets of components of the hyperfine coupling between the electron spin and the nuclear spin, namely, (1) A_{xx}, A_{yy}, $A_{zz} = 4$, 6, 38 G; and (2) A_{xx}, A_{yy}, $A_{zz} = 4$, 5, 33 G (accuracy from the spectral fitting is estimated to be ∼5%). Since a decrease in the A_{ii} component indicates a decrease in the environmental polarity of the probe,[23] the two sets of A_{ii} components will henceforth be termed "more polar" or "less polar" components, respectively.

(ii) The increase in the correlation time for the Brownian rotational diffusion motion, τ, which occurs upon adsorption, corresponds to a decrease in nitroxide mobility and indicates that the radical is interacting and binding with a surface site or with other adsorbed molecules. In the present work, the mobility falls in the range of so-called slow motion conditions of EPR: 1×10^{-9} s $< \tau < 5 \times 10^{-7}$ s.

(iii) The increased proximity of the radicals, which occurs at high loading of nitroxide onto the external surface of CaX, induces spin−spin interactions. Both dipolar (static) and Heisenberg exchange (dynamic) interactions are expected. Dipolar

interactions occur between radicals bound strongly to the surface, whereas exchange interactions take place for radicals colliding at high concentrations.[24−26] In the present case, the increase in exchange frequency, ω_{ex}, accounts well for the collapse of the hyperfine EPR lines into an increasingly more narrowed single line (e.g., Figure 4b), when the local concentration of the radicals increases. The accuracy in the evaluation of ω_{ex} is estimated to be ∼5%.

(iv) The spectra give a good fit by adding two EPR components, one arising from the radicals bound strongly at the surface (more polar environment−low mobility) and a second due to radicals in the fluid medium surrounded by ketone molecules (less polar medium−high mobility). The partitioning of the radicals in the two different environments (in percentage) was evaluated by computing the two components and adding them to each other to fit the spectra.

The main parameters (more polar or less polar component, τ, ω_{ex}, and percentage of the components) are reported in the figure at the side of each spectrum.

The main findings, based on the spectral analysis of the spectra in Figure 4 and on the computed parameters described above, were as follows:

(1) In the absence of ketone at low loading (0.01%), the EPR of 10-DN@CaX (Figure 4a), the radicals are mainly bound to a more polar environment and possess low mobility ($\tau = 20$ ns). It is plausible that under these conditions 10-DN is bound to or is near a hole on the external surface and is interacting with a cation or some polar surface defect, such as a hydroxy group.

(2) Coadsorption of $\mathbf{1}_{12}$ at low 10-DN loading (0.01%) causes a partial modification of the EPR line shape: a small fraction (15%) of radicals increased their mobility ($\tau = 9$ ns) and relocated to an environment of lower polarity. We propose that this effect (more mobile, less polar sites) arises from the interaction between the ketone molecules and the nitroxide radicals, which are displaced by the ketone from the more polar sites (holes). The signal arising from the ketone−radical interaction will henceforth be termed "ketone−radical signal", whereas the signal obtained by probes at the initial (less mobile, more polar sites) binding site on the zeolite surface will be termed the "zeolite−radical signal". Evidently, a small fraction of $\mathbf{1}_{12}$ molecules interacting with the radicals were trapped at the external zeolite structure and were blocked from entering the internal surface during the time scale of the measurements.

(3) The relative fraction of the "ketone−radical" signal increased significantly by coadsorption of 10-DN and $\mathbf{1}_{15}$, which is expected, since both 10-DN and most of the $\mathbf{1}_{15}$ are adsorbed on the external CaX surface at the beginning of the measurement. However, it is noteworthy that the radicals interacting with the ketone molecules (in a less polar environment) retained slow mobility ($\tau = 9$ ns). It is plausible that the restricted motion of the radical/molecule aggregates was due to both the large sizes of both 10-DN and $\mathbf{1}_{15}$ and also to hydrophilic and hydrophobic interactions between 10-DN and $\mathbf{1}_{15}$.

(4) At higher 10-DN loading (1%), the "zeolite−radical" signal did not change significantly in the absence of ketone molecules (Figure 4b), except that the spectrum displayed a small line broadening due to weak dipolar interactions among radicals at the surface. Therefore, the 10-DN molecules do not

(22) Schneider, D. J.; Freed, J. H. In *Biological Magnetic Resonance. Spin Labeling. Theory and Applications*; Berliner L. J., Reuben, J., Eds.; Plenum Press: New York, 1989; Vol. 8, p 1.

(23) (a) Janzen, E. G. *Top. Stereochem.* **1971**, *6*, 117. (b) Ottaviani, M. F.; Martini, G.; Nuti, L. *Magn. Reson. Chem.* **1987**, *25*, 897.

(24) Plachy, W.; Kivelson, D. *J. Chem. Phys.* **1967**, *47*, 3312.

(25) Aizawa, M.; Komatsu, T.; Nakagawa, T. *Bull. Chem. Soc. Jpn.* **1979**, *52*, 980. Aizawa, M.; Komatsu, T.; Nakagawa, T. *Bull. Chem. Soc. Jpn.* **1980**, *53*, 975.

(26) Sackmann, E.; Träuble, T. *J. Am. Chem. Soc.* **1972**, *94*, 4482, 4492 and 4499.
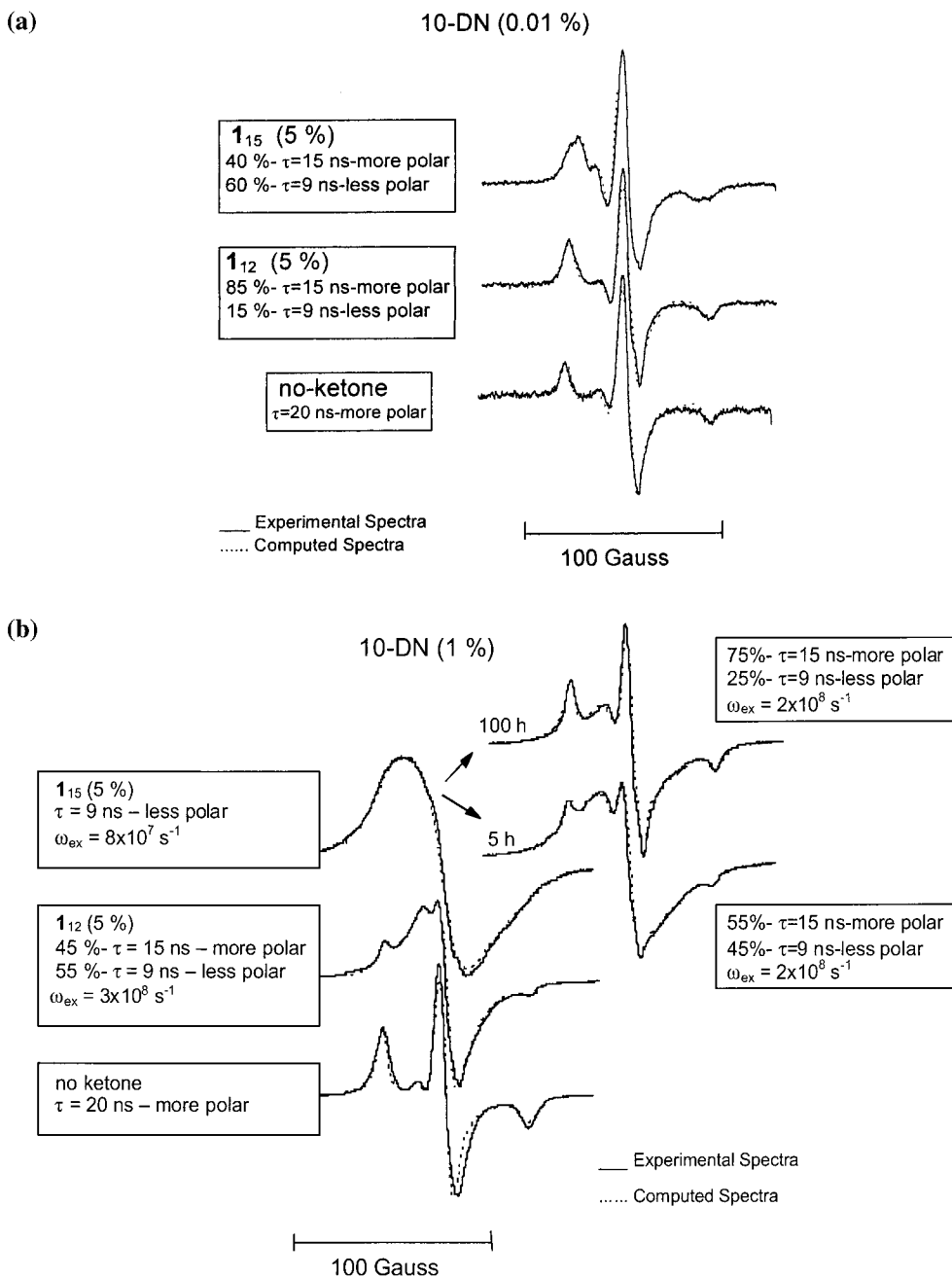
(a)   10-DN (0.01 %)

$\mathbf{1}_{15}$ (5 %)
40 %- τ=15 ns-more polar
60 %- τ=9 ns-less polar

$\mathbf{1}_{12}$ (5 %)
85 %- τ=15 ns-more polar
15 %- τ=9 ns-less polar

no-ketone
τ=20 ns-more polar

____ Experimental Spectra
...... Computed Spectra

|———— 100 Gauss ————|

(b)   10-DN (1 %)

75%- τ=15 ns-more polar
25%- τ=9 ns-less polar
ω_{ex} = 2x10^8 s^{-1}

100 h

$\mathbf{1}_{15}$ (5 %)
τ = 9 ns – less polar
ω_{ex} = 8x10^7 s^{-1}

5 h

$\mathbf{1}_{12}$ (5 %)
45 %- τ = 15 ns – more polar
55 %- τ = 9 ns – less polar
ω_{ex} = 3x10^8 s^{-1}

55%- τ=15 ns-more polar
45%- τ=9 ns-less polar
ω_{ex} = 2x10^8 s^{-1}

no ketone
τ = 20 ns – more polar

____ Experimental Spectra
...... Computed Spectra

|———— 100 Gauss ————|

Figure 4. EPR spectra of 10-DN adsorbed onto CaX (0.01 and 1% loading) in the absence and in the presence of $\mathbf{1}_{12}$ and $\mathbf{1}_{15}$ (5% loading). For 10-DN loading of 1%, the spectra recorded after 5 and 100 h from $\mathbf{1}_{15}$ loading are also reported. Full lines, experimental spectra (298 K); dashed lines, computed spectra: the main parameters of computation are reported beside each spectrum.
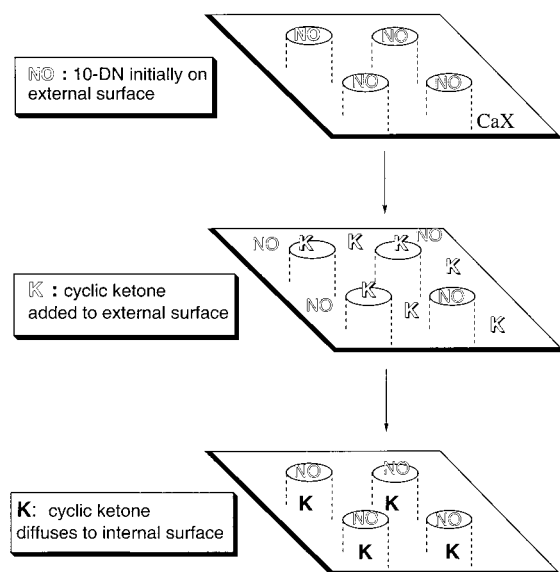
tend to aggregate and prefer to bind in a noncooperative manner to surface sites that are separated by distances of >14 Å, the estimated separation for the onset of dipolar interaction between spatially fixed radicals. It is plausible that these sites correspond to the holes' entrances on the external surface.

(5) Coadsorption of 10-DN (1%) and $\mathbf{1}_{12}$ at the CaX surface produces a spectrum which shows that a large fraction of radicals (55%) are involved in strong dynamic spin–spin interactions (ω_{ex} = 3 × 10^8 s^{-1}) resulting from molecular collisions. We propose that the spin–spin interactions arise from formation of 10-DN aggregates, where a small fraction of ketone molecules works as aggregating centers on the external surface. More than half of the 10-DN molecules are displaced from the zeolite binding sites (near or in holes) to form these aggregates, which also prevent the adsorption of a small fraction of ketones from entering the internal CaX surface. With time, the spectrum

eventually transforms into one which is essentially identical to that observed in the absence of ketone. This is because the small amount of ketone forming aggregates with 10-DN diffuses into the internal surface, leaving the 10-DN on the external surface.

(6) Coadsorption of 10-DN (1%) and $\mathbf{1}_{15}$ gave rise to a broad "ketone–radical" EPR signal (involving ~100% of radicals) characterized by lower exchange frequency (ω_{ex} = 8 × 10^7 s^{-1}) than that found for the $\mathbf{1}_{12}$ samples. A decrease in the exchange frequency corresponds to a decrease in the local concentration or rate of collisions of the radicals. A high concentration of $\mathbf{1}_{15}$ molecules is assumed to be initially localized at the external surface and to form aggregates together with the radical molecules, as in the case of $\mathbf{1}_{12}$. However, because of the larger concentration on the external surface, essentially all of the 10-DN molecules are involved in ketone–radical aggregates. The higher concentration of ketone decreases the local concentration

Scheme 4

Figure 5. (a) EPR spectra of 5-DD adsorbed onto CaX (0.01% loading) in the presence of $\mathbf{1}_{12}$ and $\mathbf{1}_{15}$ (5% loading) before irradiation; (b) variation in the intensity of the EPR signal 10-DN$-\mathbf{1}_{12}$ and 10-DN$-\mathbf{1}_{15}$ after irradiation.

of radicals in the aggregates, leading to a lower value of the exchange frequency.

(7) The spectrum of coadsorbed 10-DN (1%) and $\mathbf{1}_{15}$ changes with time. The initial broad spectrum, which is dominated by spin−spin interactions, is transformed over time into a spectrum closely resembling that of 10-DN in the absence of $\mathbf{1}_{15}$. This is shown in Figure 4b for 10-DN (1%) + $\mathbf{1}_{15}$ (5%) at $t = 5$ and 100 h (where t is the "aging" time after sample preparation). This result is similar to that described above for the behavior of the 10-DN (1%) + $\mathbf{1}_{12}$ (5%) system. The interpretation is that 10-DN is displaced from the less polar sites (aggregates with ketones) to the more polar sites (zeolite surface) as the ketone is adsorbed into the internal surface. This process allows the destruction of the 10-DN/ketone aggregates and redistribution and separation of 10-DN molecules on the external surface. These conclusions are shown schematically in Scheme 4.

5-DD (structure in Chart 2), a nitroxide probe possessing smaller alkyl chains than 10-DN, but which is still too large to be adsorbed into the internal surface, was also examined in the presence and absence of coadsorbed ketones. Coadsorption of 5-DD (0.01%) onto the CaX with $\mathbf{1}_{12}$ and $\mathbf{1}_{15}$ produced the EPR spectra shown in Figure 5. First, 5-DD in the absence of ketones shows that the radicals are bound to a more polar site and are in slow motion limit ($\tau = 10$ ns, from computation, result not shown) but undergo faster motion than 10-DN ($\tau = 20$ ns). The faster motion of 5-DD compared to 10-DN is expected, since the van der Waals interactions with the surface are weaker due to 5-DD having shorter chains compared to 10-DN. The spectrum of 5-DD did not change upon coadsorption of $\mathbf{1}_{12}$. This is expected, since the ketone is mainly adsorbed on the internal surface of CaX and does not perturb 5-DD adsorption at the external zeolite sites (more polar environment).

However, the spectrum (Figure 5) produced by coadsorption of 5-DD (0.01%) and $\mathbf{1}_{15}$ is strikingly different from any of the spectra shown in Figure 4. The spectrum consists mainly of a sharp three-line spectrum, characteristic of a nitroxide in fast motion ($\tau = 7 \times 10^{-11}$ s) in a low-polarity environment. This three-line signal is analogous to that obtained in previous work by loading 4-oxo-Tempo (structure in Chart 2) in pentasil zeolites in the presence of dibenzyl ketones. Computation showed that ∼85% of the radicals are sited in a lower polarity environment, which allows fast motion, and that ∼15% of the
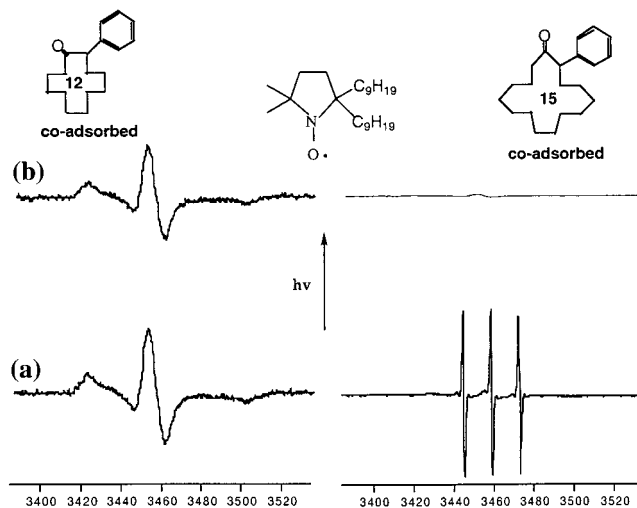
radicals are sited in a higher polarity environment, which allows slow motion.

In an attempt to correlate the photochemistry with the EPR results, 5-DD was coadsorbed with $\mathbf{1}_{12}$@CaX and $\mathbf{1}_{15}$@CaX and the systems were photolyzed. The spectrum of 5-DD did not change significantly upon sample irradiation, although photolysis of $\mathbf{1}_{12}$@CaX does occurs. This result is expected if the ketone is adsorbed mainly on the internal surface and the nitroxide radicals are adsorbed on the external surface. On the other hand, the photolysis of $\mathbf{1}_{15}$@CaX caused the complete disappearance of the sharp EPR spectrum of 5-DD. This is also expected, since the ketone is present on the external surface along with the nitroxide radicals, which are excellent scavengers of carbon-centered radicals and biradicals. Photolysis of $\mathbf{1}_{15}$@CaX produced biradicals $\mathbf{B}_{15}$ that are scavenged by the nitroxide radicals before recombining to produce $\mathbf{C}_{15}$ (Scheme 1). Consequently, the spectrum of 5-DD disappeared upon photolysis. A similar behavior was found for the irradiation with 10-DN and the cyclic ketones.

Solid-State ^{13}C NMR of $\mathbf{1}_{12}$@CaX and $\mathbf{1}_{15}$@CaX. Figure 6 shows the ^{13}C NMR spectrum of $\mathbf{1}_{15}$ in solvent CDCl$_3$ and adsorbed onto CaX, both freshly prepared and after 270 h of aging. In CDCl$_3$, the assignment of signals is as follows: 212 ppm, carbonyl carbon; 139, 129−127 ppm, phenyl carbons; 58 ppm, α-tertiary carbons; 41 ppm, α-methylene carbons; 32, 27, 26, and 23 ppm, other methylene carbons. The ^{13}C NMR spectrum of $\mathbf{1}_{12}$ in CDCl$_3$ was similar to that of $\mathbf{1}_{15}$ except for the details of the absorptions in the methylene region.

The solid-state ^{13}C NMR of $\mathbf{1}_{15}$ (5% loading) on CaX was recorded by applying CP-MAS. As expected for solid-state spectra, the peaks were somewhat broadened, and the weaker signals were difficult to distinguish from the noise level. However, it is clear that the phenyl carbon absorptions at 127−129 ppm strongly decreased in intensity, in relation to the methylene carbon's adsorption at 26−27 ppm, whose intensity was enhanced. After 270 h, new peaks at 54 and 44 ppm, and at high-field 17, 13, and 7 ppm appeared which are due to an upfield shift of the signals of the methylene carbon peaks. These new peaks did not appear with time when $\mathbf{1}_{15}$ was loaded on NaX. The new signals did not appear with time when $\mathbf{1}_{12}$ was loaded on CaX under similar conditions.
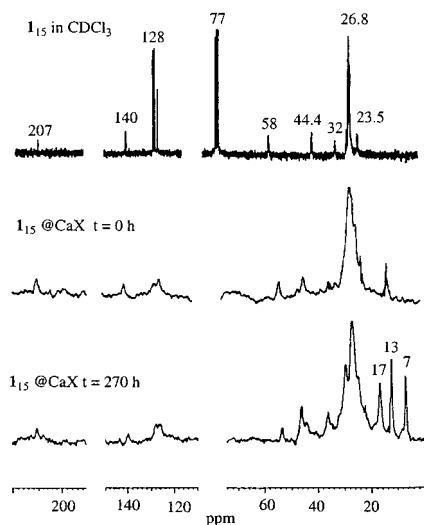
Figure 6. ^{13}C NMR spectra of $\mathbf{1}_{15}$ in CDCl$_3$ and adsorbed onto CaX (3% loading), immediately after loading, and after 270 h from loading.

Table 1. IR Absorption of 2-Phenylcycloalkanones on CaX

	maximum (cm^{-1})		
	$\nu_{sym}(CH^2)$	$\nu_{asym}(CH^2)$	$\nu(C{=}O)$
mechanical mixture of $\mathbf{1}_{12}$/CaX	2934	2862	1700
$\mathbf{1}_{12}$ internal surface[a]	2934	2862	1696, 1684
mechanical mixture of $\mathbf{1}_{15}$/CaX	2927	2854	1701
$\mathbf{1}_{15}$ external surface[a]	2929	2859	1702
$\mathbf{1}_{15}$ internal surface[b]	2931	2861	1693

[a] Spectrum taken immediately after sample preparation. [b] Spectrum taken after 270 h at room temperature.

Single-crystal X-ray analysis of $\mathbf{1}_{15}$ showed[27] that the phenyl ring is oriented toward the outer edge of the C$_{15}$ ring. In this conformation, the interaction between the phenyl ring and the methylene chain is small and the phenyl group has negligible effect on the chemical shifts of the methylene carbon atoms. The shift to high field upon inclusion into the CaX channels is consistent with a modification of the conformation of $\mathbf{1}_{15}$ which forces the phenyl ring plane to overlap with the methylene chain. In such a conformation, some of the methylene carbons will be shielded by the phenyl ring, so that their signals will be shifted to higher field. This structural change is plausible on the basis of the van der Waals interaction between CaX polar surface and the carbonyl group. The absence of these shifts for $\mathbf{1}_{12}$ is consistent with greater steric constraints which require a more compact conformation for $\mathbf{1}_{15}$ in the supercages.

FT-IR Spectra of $\mathbf{1}_{12}$@CaX and $\mathbf{1}_{15}$@CaX. The FT-IR spectra of mechanical mixtures of CaX and $\mathbf{1}_{12}$ and $\mathbf{1}_{15}$ were recorded and compared to the spectra of $\mathbf{1}_{12}$@CaX and $\mathbf{1}_{15}$@CaX. Table 1 reports the adsorption maximums for the methylene groups (symmetric and antisymmetric stretching frequencies ν_{sym} and ν_{asym}, respectively) and for the carbonyl (C=O) stretching frequency of the various samples. When $\mathbf{1}_{15}$ was adsorbed at the external CaX surface (spectrum taken shortly after sample preparation at room temperature), the IR spectrum was similar to that of the mixture of $\mathbf{1}_{15}$ with CaX, with the exception of a broadening of the carbonyl and a 5-cm^{-1} blue-shift of the ν_{sym} of the methylene protons. When $\mathbf{1}_{15}$ is adsorbed into the internal surface of CaX (spectrum taken and the sample allowed to stand at room temperature for 270 h),

the carbonyl vibration shows a $\sim$10-cm^{-1} red-shift, while the ν_{sym}, and ν_{asym}, of CH$_2$ show 4- and 7-cm^{-1} blue-shifts, respectively.

It has been reported that the red-shifts of the carbonyl vibration are a result of an interaction of the carbonyl O atom with charge-compensating cations at the zeolite surface[28a] and that the constraints exerted by the CaX walls on the methylene chain increased the force constant that caused the blue-shift of the corresponding vibrations.[28b] This is the case in which $\mathbf{1}_{15}$ molecules are adsorbed into the internal surface of CaX. Thus, the IR results indicate that the ketone molecules in the supercages are tightly bound, a result consistent with the ^2H NMR results.

The major difference between the mechanical $\mathbf{1}_{12}$/CaX mixture and $\mathbf{1}_{12}$@CaX was a red-shift of the carbonyl adsorption, which is consistent with the interaction of the carbonyl group with charge-compensating cations in the zeolite supercages and less tight binding within the supercages compared to $\mathbf{1}_{15}$@CaX.

Conclusions

A combined NMR-EPR-IR analysis of $\mathbf{1}_{12}$@CaX and $\mathbf{1}_{15}$@CaX, both in the absence and in the presence of other molecules, such as benzene and nitroxide radicals, provided information on the supramolecular structure and dynamics of these systems. The results demonstrate that the initial supramolecular structure of the $\mathbf{1}_{12}$@CaX system involves ketone molecules on the internal surface and that the initial $\mathbf{1}_{15}$@CaX system involves ketones on the external surface. The supramolecular structure of the $\mathbf{1}_{12}$@CaX is time independent over many hours and is not significantly dependent on loading. The supramolecular structure of the $\mathbf{1}_{15}$@CaX is time and loading dependent. The initial structure involves ketone molecules adsorbed on the external surface, which diffuse into the internal surface with time. The diffusion into the internal surface is accelerated by heating or by an increase in loading. These results are consistent with the proposed interpretation of the photochemistry of $\mathbf{1}_{12}$@CaX and $\mathbf{1}_{15}$@CaX (Scheme 1).

The results also provide information on the structure and dynamics of $\mathbf{1}_{12}$@CaX and $\mathbf{1}_{15}$@CaX systems in the presence of coadsorbed guests specifically located on the external (nitroxides) and internal (benzene) surfaces.

^2H NMR shows that C$_6$$^2H_6$@CaX is adsorbed exclusively on the internal surface. The time dependence of the ^2H NMR spectrum of C$_6$$^2H_6$@CaX is different in the absence and presence of $\mathbf{1}_{12}$ and $\mathbf{1}_{15}$. Reorganization of the benzene molecules can be deduced from the time dependence of the spectra (Schemes 2 and 3). In the absence of added ketones, the benzene molecules (at 2% loading) eventually occupy supercages individually and demonstrate fast mobility on the ^2H NMR time scale. In the presence of $\mathbf{1}_{12}$ (15% loading), the benzene molecules eventually occupy supercages along with the ketones and are immobile on the ^2H NMR time scale. In the presence of $\mathbf{1}_{15}$ (15% loading), two or more benzene molecules are distributed into supercages and are able to undergo rapid site exchange on the ^2H NMR time scale.

EPR shows that the nitroxides 10-DN and 5-DD are adsorbed exclusively on the external surface. Coadsorption of either nitroxide with $\mathbf{1}_{12}$ has only a minor influence on the observed EPR spectra of the nitroxides; this is because $\mathbf{1}_{12}$ is adsorbed on the internal surface of CaX and the nitroxides are adsorbed on the external surface of CaX. However, coadsorption of $\mathbf{1}_{15}$ has a major influence on the EPR spectra of the nitroxides; this

(27) Lei, X.-G., unpublished results.

(28) (a) Kubelkova, L.; Cejka, J.; Novakova, J. *Zeolites* **1991**, *11*, 48. (b) Angell, C. L.; Howell, M. V. *J. Colloid Interface Sci.* **1968**, *28*, 279.

is because both the ketone and nitroxide are adsorbed on the external surface of CaX. In the case of 10-DN, 1_{15} causes the formation of nitroxide aggregates on the external surface. With time, the aggregates redistribute over the external surface, as 1_{15} molecules diffuse into the internal surface (Scheme 4). In the case of 5-DD, the ketone does not cause aggregation but displaces the nitroxide to a less polar site on the external surface at which time the nitroxide demonstrates fast mobility. The difference in behavior between the two nitroxides and 1_{15} is attributed to the differences in van der Waals interactions between the chains of the two nitroxides and 1_{15}. Both nitroxides are scavenged by biradicals produced by photolysis of 1_{15}. Neither nitroxide is scavenged by the biradicals produced by the photolysis of 1_{12}, as expected from the supramolecular structure of the systems.

^{13}C NMR analysis indicates a variation of conformation of 1_{15} internally adsorbed by CaX, corresponding to the rotation of the phenyl groups toward the methylene groups. A blue-shift in the methylene peaks and a red-shift in the carbonyl peak in the FT-IR spectra occurred upon adsorption of 1_{12} and 1_{15} to the internal surface, due to the effect of cations and steric hindrance of the ketone molecules hosted in CaX super-cages.

Thus, a comparative analysis of the NMR-EPR-IR spectra of 1_{12}@CaX 1_{15}@CaX provides detailed information of the adsorption behavior (supramolecular structure, interactions, kinetics) of these cyclic ketones at the external/internal CaX surface. The internalization of 1_{15} may be depicted as the behavior of "an octopus entering a cave". Like the octopus, the ketone molecules adapted their conformation to the internal CaX structure and squeezed into the zeolite channels to finally reach an equilibrium structure within the supercages.

JA002844O